Operator Norm-based Statistical Linearization to Bound the First Excursion Probability of Nonlinear Structures Subjected to Imprecise Stochastic Loading

Matthias G.R. Faes*, M.ASCE[1], Vasileios C. Fragkoulis[2], Peihua Ni, S.M.ASCE[3], Danko J. Jerez, S.M.ASCE[4], Marcos A. Valdebenito, Aff.M.ASCE[5], and Michael Beer, M.ASCE[6]

[1]Post-doctoral Fellow, KU Leuven, Department of Mechanical Engineering, Technology campus De Nayer, Jan De Nayerlaan 5, St.-Katelijne-Waver, Belgium; Alexander von Humboldt fellow, Institute for Risk and Reliability, Leibniz Univ. Hannover, Callinstr. 34, Hannover 30167, Germany. E-mail: matthias.faes@kuleuven.be

[2]Post-doctoral Fellow, Institute for Risk and Reliability, Leibniz Univ. Hannover, Callinstr. 34, Hannover 30167, Germany. E-mail: fragkoulis@irz.uni-hannover.de

[3]PhD Student, Institute for Risk and Reliability, Leibniz Univ. Hannover, Callinstr. 34, Hannover 30167, Germany. E-mail: peihua.ni@irz.uni-hannover.de

[4]PhD Student, Institute for Risk and Reliability, Leibniz Univ. Hannover, Callinstr. 34, Hannover 30167, Germany. E-mail: danko.jerez@irz.uni-hannover.de

[5]Professor, Faculty of Engineering and Sciences, Universidad Adolfo Ibáñez, Av. Padre Hurtado 750, 2562340 Viña del Mar, Chile. E-mail: marcos.valdebenito@uai.cl

[6]Professor and Head, Institute for Risk and Reliability, Leibniz Univ. Hannover, Callinstr. 34, Hannover 30167, Germany; Part-Time Professor, Institute of Risk and Uncertainty, Univ. of Liverpool, Peach St., Liverpool L69 7ZF, UK; Guest Professor, Shanghai Institute of Disaster Prevention and Relief, Tongji Univ., Shanghai 200092, China. E-mail: beer@irz.uni-hannover.de

ABSTRACT

This paper presents a highly efficient approach for bounding the responses and probability of failure of nonlinear models subjected to imprecisely defined stochastic loads. Typically, such

computations involve solving a nested double loop problem, where the propagation of the aleatory uncertainty has to be performed for each realization of the epistemic uncertainty. Apart from near-trivial cases, such computation is intractable without resorting to surrogate modeling schemes, especially in the context of performing nonlinear dynamical simulations. The recently introduced operator norm framework allows for breaking this double loop by determining those values of the epistemic uncertain parameters that produce bounds on the probability of failure a priori. However, the method is in its current form only applicable to linear models due to the adopted assumptions in the derivation of the involved operator norms. In this paper, the operator norm framework is extended and generalized by resorting to the statistical linearization methodology, to account for nonlinear systems. Two case studies are included to demonstrate the validity and efficiency of the proposed approach.

Keywords: Uncertainty quantification; Imprecise probabilities; Operator norm theorem; Statistical linearization

INTRODUCTION

Uncertainties about the true properties of, and loads acting on, structural systems are commonly encountered in the context of all fields of engineering, including structural dynamics. For instance, natural phenomena such as earthquakes or wind loads are especially hard to model exactly, since the corresponding dynamical loads acting on the system often cannot be described in a crisp way due to the sheer complexity of the underlying phenomena. Further, when designing structures with natural or highly engineered materials, such uncertainties may arise as well. To treat these issues effectively, stochastic processes (Shinozuka and Sato 1967, Vanmarcke and Grigoriu 1983) have been introduced as a rigorous framework to account for the aleatory uncertainties and corresponding correlations in space and time of uncertain loads and properties. This is obtained by resorting to the well-documented framework of probability theory, which is highly suited to treat aleatory uncertainties.

However, the definition of such stochastic processes may require prohibitively amounts of informative data to fully characterize the probabilistic descriptors, including the auto-correlation.

In a practical engineering context, such information may not always be available due to scarcity, incompleteness or even conflicted nature of typically available data sources. As a potential remedy, one can model the additional (epistemic) uncertainty by means of subjective probability density functions, which might be a valid approach in case sufficient reasons are present to validate the considered assumptions. However, in general, this includes unwarranted subjectivity in the analysis, which might give a wrong sense of reliability to the model. Alternatively, set theoretical approaches, such as intervals (Faes and Moens 2019b) or fuzzy numbers (Beer 2004), can be used to include the epistemic uncertainty. By imposing such set-theoretical descriptors on top of probabilistic models for the uncertainty, a full set of probabilistic models that is consistent with the lack of knowledge is considered, which allows for an objective judgement on the bounds of the system reliability. In this context, utilizing the concept of imprecise probabilities (Beer et al. 2013) provides the analyst with a concrete theoretical framework to define and compute (with such hybrid forms) the uncertainties. In structural dynamics, for instance, given a set of stochastic processes that are consistent with the epistemic uncertainty, an imprecise probabilities-based solution treatment leads to bounds on the first excursion probability. The latter not only allows to assess the sensitivity of the model reliability to the existing epistemic uncertainty, but also yields an estimate of the lower bound of the reliability.

In engineering practice, however, the effective application of such methods is typically hindered by the corresponding computational cost. In essence, the propagation of the epistemic and aleatory uncertainty has to be performed such that their effects on the reliability are kept separated (Moens and Vandepitte 2004). This gives rise to double loop approaches, where the outer loop takes care of epistemic uncertainty while the inner loop deals with aleatory uncertainty. Many efficient methods have been introduced in recent years to alleviate this computational cost; see, indicatively, Faes et al. (2021a) for a recent review paper. Examples of such approaches are based on Extended Monte Carlo simulation (Wei et al. 2019), surrogate modeling schemes (Schöbi and Sudret 2017), Bayesian probabilistic propagation (Wei et al. 2021) or Line Sampling (de Angelis et al. 2015). A recent development in this context is based on operator norm theory to decouple the double loop into

a deterministic optimization, followed by a single reliability analysis per bound on the reliability (Faes et al. 2020; 2021b), which is capable of reducing the corresponding computational cost by several orders of magnitude. However, the methods based on operator norm theory are limited to linear systems, which renders their application to realistic engineering models impossible.

In this regard, directing attention to extending the operator norm framework to nonlinear dynamical systems, a new technique is developed herein for computing moderate to large failure probabilities. This is attained by resorting to the statistical linearization methodology (Roberts and Spanos 2003, Socha 2007), which is used for defining an equivalent linear system of equations to account for the nonlinear system under consideration. Then, an operator norm theory-based solution treatment (Faes et al. 2021b) is employed to obtain the bounds on the probability of failure. Two pertinent numerical examples demonstrate the reliability of the proposed methodology.

BOUNDS ON THE RELIABILITY OF NONLINEAR DYNAMICAL SYSTEMS

Nonlinear stochastic dynamics

A nonlinear dynamical system subjected to a stochastic load $p(t, \boldsymbol{\xi})$ is represented using the Finite Element representation of the dynamical equation, by the following set of ordinary differential equations:

$$\mathbf{M}\ddot{\mathbf{q}}(t) + \mathbf{C}\dot{\mathbf{q}}(t) + \mathbf{K}\mathbf{q}(t) + \boldsymbol{\Phi}\left(\ddot{\mathbf{q}}(t), \dot{\mathbf{q}}(t), \mathbf{q}(t)\right) = \boldsymbol{\rho} p(t, \boldsymbol{\xi}), \tag{1}$$

where $\mathbf{M} \in \mathbb{R}^{n_d \times n_d}$, $\mathbf{C} \in \mathbb{R}^{n_d \times n_d}$ and $\mathbf{K} \in \mathbb{R}^{n_d \times n_d}$ represent, respectively, the mass, damping and stiffness matrices of the system, and n_d denotes the degrees of freedom in the model. Further, $\boldsymbol{\xi}$ represents a realization of a random variable vector, whereas the vector $\boldsymbol{\rho} \in \mathbb{R}^{n_d \times 1}$ links the stochastic load $p(t, \boldsymbol{\xi})$ to the appropriate degrees of freedom in the structure. The vectors $\mathbf{q} \in \mathbb{R}^{n_d}$, $\dot{\mathbf{q}} \in \mathbb{R}^{n_d}$ and $\ddot{\mathbf{q}} \in \mathbb{R}^{n_d}$ represent, respectively, the nodal displacements, velocities and accelerations, where a dot over a variable denotes differentiation with respect to time $t \in \mathbb{R}$. Finally, $\boldsymbol{\Phi}\left(\ddot{\mathbf{q}}(t), \dot{\mathbf{q}}(t), \mathbf{q}(t)\right) \in \mathbb{R}^{n_d}$ represents the nonlinear restoring force, which depends on the nodal displacement, velocity and acceleration vectors.

In Eq. (1), $p(t, \boldsymbol{\xi})$ represents the load to which the system is subjected, which in the context of

stochastic dynamical systems is usually modeled as a stochastic process. If $\phi(t, \boldsymbol{\xi})$ is a stationary zero-mean Gaussian process, it can be characterized using its power spectral density function $S_{PP}(\omega)$, where $\omega \in \mathbb{R}$ denotes the circular frequency. The Wiener-Khintchine theorem allows for the calculation of the autocorrelation function corresponding to $S_{PP}(\omega)$, and vice versa. This is attained by utilizing the Fourier transforms:

$$S_{PP}(\omega) = \frac{1}{2\pi} \int_{-\infty}^{+\infty} R_{PP}(\tau) e^{-i\omega\tau} d\tau, \quad R_{PP}(\tau) = \int_{-\infty}^{+\infty} S_{PP}(\omega) e^{i\omega\tau} d\omega, \tag{2}$$

where $R_{PP}(\tau)$ denotes the autocorrelation function with time lag $\tau \in \mathbb{R}$. Sample paths of this stochastic process can be generated, for example, by applying the Karhunen-Loève (KL) expansion (e.g., Schenk and Schuëller 2005, Stefanou 2009). In this regard, assume that the loading is applied for time T, where $t_k = (k-1)\Delta t, \ k = 1, 2, \ldots, n_T$, corresponds to time discretization with step Δt and n_T denotes the number of discrete time steps. Then, the associated discrete covariance matrix $\mathbf{R_{PP}} \in \mathbb{R}^{n_T \times n_T}$ becomes:

$$\mathbf{R_{PP}} = \begin{bmatrix} R_{P_1P_1}(0) & R_{P_1P_2}(t_1 - t_2) & \ldots & R_{P_1P_{n_T}}(t_1 - t_{n_T}) \\ R_{P_2P_1}(t_2 - t_1) & R_{P_2P_2}(0) & \ldots & R_{P_2P_{n_T}}(t_2 - t_{n_T}) \\ \vdots & \vdots & \ddots & \vdots \\ R_{P_{n_T}P_1}(t_{n_T} - t_1) & R_{P_{n_T}P_1}(t_{n_T} - t_2) & \ldots & R_{P_{n_T}P_{n_T}}(0) \end{bmatrix}. \tag{3}$$

Utilizing the matrix-vector form of the KL expansion, i.e.:

$$\mathbf{p}(\boldsymbol{\xi}) = \boldsymbol{\Psi}\boldsymbol{\Lambda}^{1/2}\boldsymbol{\xi}, \tag{4}$$

sample paths compatible with the stochastic ground acceleration are generated. In Eq. (4), $\mathbf{p}$ denotes an n_T-dimensional vector containing the sample of the loading; $\boldsymbol{\xi}$ is a realization of the random variable vector $\boldsymbol{\Xi}$, which follows an n_{KL}-dimensional standard Gaussian distribution, where n_{KL} corresponds to the number of terms retained in the KL expansion; $\boldsymbol{\Psi} \in \mathbb{R}^{n_T \times n_{KL}}$ is a matrix whose columns contain the eigenvectors associated with the largest n_{KL} eigenvalues

of the discrete covariance matrix $\mathbf{R_{PP}}$; and $\mathbf{\Lambda} \in \mathbb{R}^{n_{KL} \times n_{KL}}$ denotes a diagonal matrix whose elements contain the largest n_{KL} eigenvalues of $\mathbf{R_{PP}}$. A criterion for selecting the number of terms to be retained in the KL expansion is to find the minimum value of n_{KL}, such that $\sum_{p=1}^{n_{KL}} \lambda_p \geq p_v \sum_{p=1}^{n_T} \lambda_p$, where p_v denotes the fraction of the total variance of the underlying stochastic process that is retained by the approximate representation, and λ_p is the p-th eigenvalue of $\mathbf{R_{PP}}$ (Lee and Verleysen 2007). For a recent overview of numerical methods to solve the associated Fredholm integral eigenvalue problem in a continuous case, the reader is directed to Betz et al. (2014). Alternatively, the sample paths can also be generated using frequency domain methods, such as described in Chen and Li (2013).

In a structural engineering context, one is usually interested in finding the reliability of the structure, which is related to its performance by means of Eq. (1). Practically, the structural reliability can be quantified by its complement, i.e., the failure probability P_f. In this context, failure is encoded in the performance function $g(\boldsymbol{\xi})$, i.e., $g(\boldsymbol{\xi}) \leq 0$ indicates that the realization of values $\boldsymbol{\xi}$ leads to a structural failure. The probability of failure is calculated by solving the integral equation:

$$P_f = \int_{\boldsymbol{\xi} \in \mathbb{R}^{n_{KL}}} I_F\left(\boldsymbol{\xi}\right) f_{\boldsymbol{\Xi}}\left(\boldsymbol{\xi}\right) d\boldsymbol{\xi}, \tag{5}$$

where $f_{\boldsymbol{\Xi}}\left(\cdot\right)$ is a standard n_{KL}-dimensional Gaussian probability density function and $I_F\left(\cdot\right)$ is the indicator function, whose value is equal to one in case $g(\boldsymbol{\xi}) \leq 0$ and zero otherwise. Note, in passing, that the exact formulation of $g(\boldsymbol{\xi})$ is highly case dependent. For instance, when considering the first-passage problem, which is a classical problem in stochastic dynamics (e.g., Spanos and Kougioumtzoglou 2014, Spanos et al. 2016), $g(\boldsymbol{\xi})$ is given by:

$$g\left(\boldsymbol{\xi}\right) = 1 - \max_{i=1,\ldots,n_\eta} \left(\max_{k=1,\ldots,n_T} \left(\frac{\left|\eta_i\left(t_k, \boldsymbol{\xi}\right)\right|}{b_i} \right) \right). \tag{6}$$

In Eq. (6), $\eta_i(t_k, \boldsymbol{\xi}),\ i = 1, 2, \ldots, n_\eta$, indicates the i-th response of the system at time instant t_k (e.g., q_i or one of its time derivatives), $|\cdot|$ denotes the absolute value and b_i is a predefined threshold value above which a structural failure occurs (e.g., a maximally allowed acceleration).

The integral in Eq. (5) usually comprises a high number of dimensions, as n_{KL} may be in the order of hundreds or thousands for realistic stochastic processes. Furthermore, $g(\boldsymbol{\xi})$, and hence, $I_F(\boldsymbol{\xi})$ is only known point-wise for realizations $\boldsymbol{\xi}$ of $\boldsymbol{\Xi}$. Therefore, such an integral cannot be solved analytically. In general, simulation methods should be applied to evaluate P_f (Schuëller and Pradlwarter 2007). However, using simulation methods to calculate the probability of failure of a non-linear dynamical system can become quite challenging (Pradlwarter et al. 2007). For instance, the definition of appropriate importance sampling density functions to be used within the context of Importance Sampling might not always be trivial in this case (Au 2009). Moreover, it is highlighted that the nonlinear restoring force $\boldsymbol{\Phi}(\ddot{\mathbf{q}}(t), \dot{\mathbf{q}}(t), \mathbf{q}(t))$ in Eq. (1) hinders the determination of $\eta_i(t_k), i = 1, 2, \ldots, n_\eta, k = 1, 2, \ldots, n_T$, since its presence necessitates the employment of pertinent numerical algorithms, such as these based on Newmark schemes (Chopra 1995). In particular, combining simulation algorithms with these nonlinear solvers potentially leads to solution frameworks of increased computational cost.

Imprecise stochastic dynamical analysis

The characterization of the stochastic process $p(t, \boldsymbol{\xi})$ in Eq. (1) in terms of its power spectral density, or autocorrelation function, usually relies on a prescribed model. This, in turn, depends on a number of parameters, which are grouped in a vector $\boldsymbol{\theta} \in \mathbb{R}^{n_\theta}$. In this case, the parameters that determine the covariance matrix $\mathbf{R_{PP}}(\tau|\boldsymbol{\theta})$ reflect some specific characteristics of the process, such as dominant frequencies, amplitude, etc. When selecting the appropriate value of these quantities, the analyst may be faced with considerable uncertainty, such as lack of knowledge, vague or ambiguous information, etc., which leads to epistemic uncertainty concerning the correct parameter value. Therefore, instead of selecting a crisp value, it is often preferred to explicitly account for this epistemic uncertainty by resorting to non-traditional models for uncertainty quantification (Beer et al. 2013).

In this regard, it is herein assumed that the epistemic uncertainty in the definition of $\boldsymbol{\theta}$ can be bounded by an interval, i.e., $\boldsymbol{\theta} \in \boldsymbol{\theta}^I = [\underline{\boldsymbol{\theta}}, \overline{\boldsymbol{\theta}}]$, where $\underline{\boldsymbol{\theta}}$ and $\overline{\boldsymbol{\theta}}$ denote, respectively, the lower and upper bound between which the *true* parameter value is believed to lie. Techniques to infer these

bounds based on limited data have been reported; see, indicatively, Imholz et al. (2020). Taking these uncertainties explicitly into account, Eq. (1) becomes:

$$\mathbf{M}\ddot{\mathbf{q}}(t) + \mathbf{C}\dot{\mathbf{q}}(t) + \mathbf{K}\mathbf{q}(t) + \mathbf{\Phi}\left(\ddot{\mathbf{q}}(t), \dot{\mathbf{q}}(t), \mathbf{q}(t)\right) = \boldsymbol{\rho} p(t, \boldsymbol{\xi}, \boldsymbol{\theta}^I). \tag{7}$$

Close inspection of Eq. (7) reveals that both intervals and random variables are present. The fact that the input parameters of the stochastic loading model are described by means of intervals has important implications on the evaluation of the structural reliability of the model under consideration. In particular, both loading and the structural system responses become interval stochastic processes (Faes and Moens 2019a). This, in turn, leads to an interval valued performance function, which causes the failure probability to become interval valued as well. Therefore, instead of calculating a single probability of failure associated with the structure (using Eq. (5)), given the epistemic uncertainty represented by $\boldsymbol{\theta}^I$, one has to estimate the bounds on P_f. These bounds are calculated by solving the optimization problems:

$$\underline{P}_f = \min_{\boldsymbol{\theta} \in \boldsymbol{\theta}^I} \left(P_f(\boldsymbol{\theta})\right) = \min_{\boldsymbol{\theta} \in \boldsymbol{\theta}^I} \left(\int_{\boldsymbol{\xi} \in \mathbb{R}^{nKL}} I_F\left(\boldsymbol{\xi}, \boldsymbol{\theta}\right) f_{\boldsymbol{\Xi}}\left(\boldsymbol{\xi}\right) d\boldsymbol{\xi} \right), \tag{8}$$

$$\overline{P}_f = \max_{\boldsymbol{\theta} \in \boldsymbol{\theta}^I} \left(P_f(\boldsymbol{\theta})\right) = \max_{\boldsymbol{\theta} \in \boldsymbol{\theta}^I} \left(\int_{\boldsymbol{\xi} \in \mathbb{R}^{nKL}} I_F\left(\boldsymbol{\xi}, \boldsymbol{\theta}\right) f_{\boldsymbol{\Xi}}\left(\boldsymbol{\xi}\right) d\boldsymbol{\xi} \right). \tag{9}$$

In general, the solution of the optimization problems defined in Eqs. (8) and (9) is extremely demanding from a computational perspective. Specifically, as pointed out earlier, the solution of the reliability problem for nonlinear dynamical systems is rather cumbersome. In addition, solving the corresponding optimization problems is not straightforward, since this constitutes a double loop problem, where the inner loop comprises probability calculation, while the outer loop explores the possible values of the parameters $\boldsymbol{\theta}$. Hence, besides considering near-trivial simulation models, such computation is intractable without resorting to surrogate modelling strategies (Faes et al. 2019).

OPERATOR NORM THEORY AS A TOOL TO DECOUPLE THE DOUBLE LOOP

A highly efficient operator norm theory-based approach to decouple the double loop associated with the solution of Eqs. (8) and (9) has already been developed by some of the authors of the present paper (Faes et al. 2021b; 2020). In this section, a concise presentation of the results in Faes et al. (2021b, 2020) is provided for completeness. Then, directing attention to computing the bounds on the probability of failure of the nonlinear system given by Eq. (1), a novel methodology is proposed, which is based on the combination of the statistical linearization method (Roberts and Spanos 2003) with the theoretical framework described above.

Linear problems

The operator norm method introduced in Faes et al. (2021b, 2020), specifically focuses on models whose relation between the response $\boldsymbol{\eta}$ and the uncertain inputs $\boldsymbol{\theta}$ and $\boldsymbol{\xi}$ is recast into:

$$\boldsymbol{\eta}(\boldsymbol{\theta}, \boldsymbol{\xi}) = \mathbf{A}\mathbf{B}(\boldsymbol{\theta})\boldsymbol{\xi}. \tag{10}$$

In Eq. (10), $\mathbf{A} : \mathbb{R}^{n_d} \mapsto \mathbb{R}^{n_\eta}$ denotes a continuous linear map that represents the translation of the model input to the responses of interest, whereas $\mathbf{B} : \mathbb{R}^{n_{KL}} \mapsto \mathbb{R}^{n_d}$ is a linear map that transforms the random vector $\boldsymbol{\xi}$ to the sample paths of the stochastic process which serves as model input. For instance, using the KL series expansion, $\mathbf{B}$ is given in its discrete form as:

$$\mathbf{B} = \boldsymbol{\Psi}\boldsymbol{\Lambda}^{1/2}, \tag{11}$$

where $\boldsymbol{\Psi}$ and $\boldsymbol{\Lambda}$ are the matrices which contain, respectively, the eigenvectors and eigenvalues of the matrix $\mathbf{R_{PP}}$ (see also section "Bounds on the reliability of nonlinear dynamical systems").

Considering the linear map defined in Eq. (10) and also defining $\mathbf{D}(\boldsymbol{\theta}) = \mathbf{A}\mathbf{B}(\boldsymbol{\theta})$ for simplicity, it can be shown that the inequality:

$$\|\mathbf{D}(\boldsymbol{\theta})\boldsymbol{\xi}\|_{p_1} \leq |c| \|\boldsymbol{\xi}\|_{p_2}, \tag{12}$$

with $\|\cdot\|_p$ denoting a certain L_p norm, always holds. In essence, this equation states that the length of the uncertain model input $\boldsymbol{\xi}$ quantified via a prescribed L_{p_i} norm, can be amplified by a factor c towards the model responses $\boldsymbol{\eta}$ when applying the linear mapping defined by $\mathbf{D}(\boldsymbol{\theta})$. A measure for *how much* a certain deterministic linear map $\mathbf{D}(\boldsymbol{\theta})$ increases the length of the uncertain model input $\mathbf{v}$ in the maximum case, is given by the operator norm $\|\mathbf{D}(\boldsymbol{\theta})\|_{p_1,p_2}$, which is defined in a deterministic sense (i.e., for one realization of the uncertain parameters) as:

$$\|\mathbf{D}(\boldsymbol{\theta})\|_{p_1,p_2} = \inf\left\{c \geq 0 : ||\mathbf{D}(\boldsymbol{\theta})\mathbf{v}||_{p_1} \leq |c| \cdot \|\mathbf{v}\|_{p_2}, \forall \mathbf{v} \in \mathbb{R}^{n_v}\right\}, \tag{13}$$

or, equivalently:

$$\|\mathbf{D}(\boldsymbol{\theta})\|_{p_1,p_2} = \sup\left\{\frac{\|\mathbf{D}(\boldsymbol{\theta})\mathbf{v}\|_{p_1}}{\|\mathbf{v}\|_{p_2}} : \mathbf{v} \in \mathbb{R}^{n_v} \text{ with } \mathbf{v} \neq 0\right\}. \tag{14}$$

Clearly, the calculation of a specific value $\|\mathbf{D}(\boldsymbol{\theta})\|_{p_1,p_2}$ depends on the choice of p_1 and p_2. The interested reader is directed to Faes et al. (2021b, 2020) for an analytical presentation of the method and for guidance on the optimal selection of p_1 and p_2; and to Faes and Valdebenito (2020, 2021) for a practical application of the framework in the context of reliability-based design optimization.

In case of calculating first excursion probabilities, taking into account Eq. (6), experience shows that selecting $p_1 \to \infty$ and $p_2 = 2$ provides with exact results on which parameter realizations of $\boldsymbol{\theta}$ yield extrema in P_f. This happens since the operator norm $\|\mathbf{D}(\boldsymbol{\theta})\|_{\infty,2}$ describes the amount of 'energy' amplification in the random signal towards the 'extremes' of the responses $\boldsymbol{\eta}_i$, and hence, its corresponding effect on P_f. Thus, it is readily seen that finding those values of the epistemic uncertain parameters $\boldsymbol{\theta}$ that minimize and maximize, respectively, $\|\mathbf{D}(\boldsymbol{\theta})\|_{\infty,2}$ also provides with the realizations that minimize and maximize P_f. Hence, the double loop that is presented in Eqs. (8) and (9) can be efficiently decoupled, first, by determining $\boldsymbol{\theta}^U$ via:

$$\boldsymbol{\theta}^U = \underset{\boldsymbol{\theta}\in\boldsymbol{\theta}^I}{\operatorname{argmax}} \|\mathbf{D}(\boldsymbol{\theta})\|_{\infty,2} \tag{15}$$

to find the parameters that yield $\overline{P}_f$, and then, by determining $\boldsymbol{\theta}^L$ via:

$$\boldsymbol{\theta}^L = \underset{\boldsymbol{\theta}\in\boldsymbol{\theta}^I}{\operatorname{argmin}} \|\mathbf{D}(\boldsymbol{\theta})\|_{\infty,2} \tag{16}$$

to find the parameters that yield $\underline{P}_f$. Next, the bounds on P_f, i.e., $\underline{P}_f$ and $\overline{P}_f$, are obtained by solving Eq. (5) twice, corresponding to $\boldsymbol{\theta}^U$ and $\boldsymbol{\theta}^L$. It is noted that depending on the convexity of the problem under consideration, any pertinent optimization solver can be employed to solve Eqs. (15) and (16). Further, it is readily seen that recasting the problem in the form given by Eq. (10) is critical for the application of the method. In essence, this means that the underlying model must be linear, and that the aleatory uncertainty can only be present in the load description (Faes et al. 2021b). This feature of the method hinders its direct application to nonlinear systems defined by Eq. (7). Nevertheless, this limitation is addressed in the following by resorting to the statistical linearization method, i.e., by defining an equivalent linear system for the nonlinear system of Eq. (7).

Statistical linearization methodology

In this section, a concise presentation of the statistical linearization methodology is provided for completeness. The main objective of the method is to replace the originally considered nonlinear system with an equivalent linear one and minimize (in some sense) the difference between the two systems. Clearly, the readily available solution frameworks for treating the equivalent linear system are used to estimate the stochastic response of its nonlinear counterpart. In general, several variations of the method have been used to solve approximately and efficiently nonlinear stochastic differential equations associated with engineering applications; see, indicatively, Fragkoulis et al. (2016); Kougioumtzoglou et al. (2017); Fragkoulis et al. (2019); Spanos and Malara (2020); Pasparakis et al. (2021); Ni et al. (2021) and references therein. Its extensive utilization in stochastic dynamics is associated with its capacity to treat a wide range of nonlinear behaviors in a straightforward manner.

In this regard, the statistical linearization method is invoked herein to alleviate the computational

burden associated with Eq. (6). For the application of the method, the nonlinear system in Eq. (1) is replaced by an equivalent linear system of the form:

$$(\mathbf{M} + \mathbf{M}_e)\,\ddot{\mathbf{q}}(t) + (\mathbf{C} + \mathbf{C}_e)\,\dot{\mathbf{q}}(t) + (\mathbf{K} + \mathbf{K}_e)\,\mathbf{q}(t) = \boldsymbol{\rho} p(t, \boldsymbol{\xi}). \tag{17}$$

In Eq. (17), $\mathbf{M}_e$, $\mathbf{C}_e$ and $\mathbf{K}_e$ denote, respectively, the mass, damping and stiffness $n_d \times n_d$ matrices of the equivalent linear system that account for neglecting the nonlinearity from Eq. (1) . Next, the error $\boldsymbol{\varepsilon} \in \mathbb{R}^{n_d}$ is defined as the difference between Eqs. (1) and (17), i.e.:

$$\boldsymbol{\varepsilon} = \boldsymbol{\Phi}\left(\ddot{\mathbf{q}}(t), \dot{\mathbf{q}}(t), \mathbf{q}(t)\right) - \mathbf{M}_e\ddot{\mathbf{q}}(t) - \mathbf{C}_e\dot{\mathbf{q}}(t) - \mathbf{K}_e\mathbf{q}(t), \tag{18}$$

and its mean square is minimized. Note that although several criteria are available for minimizing $\boldsymbol{\varepsilon}$ (e.g., Socha 2007, Elishakoff and Andriamasy 2012), adopting a mean square error minimization in conjunction with the Gaussian assumption for the system response probability density functions (Roberts and Spanos 2003) facilitates the determination of the equivalent linear system in Eq. (17). Specifically, the elements of matrices $\mathbf{M}_e$, $\mathbf{C}_e$ and $\mathbf{K}_e$ are given in closed form by:

$$m_{ij}^e = \mathbb{E}\left[\frac{\partial \boldsymbol{\Phi}_i}{\partial \ddot{q}_j}\right], \quad c_{ij}^e = \mathbb{E}\left[\frac{\partial \boldsymbol{\Phi}_i}{\partial \dot{q}_j}\right], \quad k_{ij}^e = \mathbb{E}\left[\frac{\partial \boldsymbol{\Phi}_i}{\partial q_j}\right], \tag{19}$$

where $\mathbb{E}[\cdot]$ is the expectation operator and the indices $i, j = 1, 2, \ldots, n_d$ denote the corresponding element of the $n_d \times n_d$ matrices and n_d-dimensional vectors.

Next, note that the equivalent linear system response variance is also required to compute the elements of the equivalent matrices given by Eq. (19). This is attained by employing either a time- or a frequency-domain solution framework (Roberts and Spanos 2003, Fragkoulis et al. 2016, Kougioumtzoglou et al. 2017). For instance, following the latter, the system response variance is determined by resorting to the input-output relationship of random vibration theory:

$$\mathbf{S}_{\mathbf{qq}}(\omega) = \boldsymbol{\alpha}(\omega)\mathbf{S}_{\mathbf{PP}}(\omega)\boldsymbol{\alpha}^{\mathrm{T}*}(\omega), \tag{20}$$

where $\mathbf{S_{qq}}(\omega)$ and $\mathbf{S_{PP}}(\omega)$ denote, respectively, the response and excitation power spectrum, and 'T$*$' corresponds to the conjugate transpose matrix operator. Further, $\boldsymbol{\alpha}(\omega)$ is the frequency response function matrix of the equivalent system in Eq. (17), i.e.:

$$\boldsymbol{\alpha}(\omega) = \left[-\omega^2(\mathbf{M}+\mathbf{M}_e) + i\omega(\mathbf{C}+\mathbf{C}_e) + (\mathbf{K}+\mathbf{K}_e)\right]^{-1}, \tag{21}$$

where 'i' is the imaginary unit. Thus, taking into account Eqs. (20) and (21), the system response variance is determined by:

$$\mathbb{E}\left[q_i^2(t)\right] = \int_{-\infty}^{\infty} S_{q_iq_i}(\omega)\mathrm{d}\omega,\ \mathbb{E}\left[\dot{q}_i^2(t)\right] = \int_{-\infty}^{\infty} \omega^2 S_{q_iq_i}(\omega)\mathrm{d}\omega,\ \mathbb{E}\left[\ddot{q}_i^2(t)\right] = \int_{-\infty}^{\infty} \omega^4 S_{q_iq_i}(\omega)\mathrm{d}\omega, \tag{22}$$

where $S_{q_iq_i}(\omega)$, $i = 1, 2, \ldots, n_d$, are the diagonal elements of the system response spectrum $\mathbf{S_{qq}}(\omega)$. Clearly, Eq. (19) and Eq. (22) define a coupled set of nonlinear equations to be solved for determining $\mathbf{M}_e, \mathbf{C}_e$ and $\mathbf{K}_e$. For its solution, the following iterative scheme is used. First, the equivalent parameter matrices in Eq. (17) are set equal to null matrices. Then, initial values for the response variance are computed by Eq. (22). Next, the latter are used in conjunction with Eq. (19) to update the values for $\mathbf{M}_e, \mathbf{C}_e$ and $\mathbf{K}_e$. The last two steps are repeated until convergence.

Note that, depending on the form of nonlinearity $\boldsymbol{\Phi}\left(\ddot{\mathbf{q}}(t), \dot{\mathbf{q}}(t), \mathbf{q}(t)\right)$ in Eq. (7), the matrices $\mathbf{M}+\mathbf{M}_e, \mathbf{C}+\mathbf{C}_e$ and $\mathbf{K}+\mathbf{K}_e$ in the equivalent system are no longer necessarily symmetric. Further, note that matrix $\mathbf{C}+\mathbf{C}_e$ represents a 'full' damping matrix. Therefore, commonly applied solution schemes based on convolution, as described in Chopra (1995) are not directly applied. A potential solution hereto is to recast the equations into a state-space form (Chopra 1995; Jensen and Valdebenito 2007):

$$\mathbf{M}^*\ddot{\mathbf{q}}(t) + \mathbf{K}^*\mathbf{q}(t) = \mathbf{P}^*(t, \boldsymbol{\xi}), \tag{23}$$

where $\mathbf{M}^* \in \mathbb{R}^{2n_d \times 2n_d}$, $\mathbf{K}^* \in \mathbb{R}^{2n_d \times 2n_d}$ and $\mathbf{P}^* \in \mathbb{R}^{2n_d \times 1}$ are block matrices given by:

$$\mathbf{M}^* = \begin{bmatrix} \mathbf{0} & \mathbf{M} + \mathbf{M}_e \\ \mathbf{M} + \mathbf{M}_e & \mathbf{C} + \mathbf{C}_e \end{bmatrix}, \quad \mathbf{K}^* = \begin{bmatrix} -(\mathbf{M} + \mathbf{M}_e) & \mathbf{0} \\ \mathbf{0} & \mathbf{K} + \mathbf{K}_e \end{bmatrix}, \quad \mathbf{P}^* = \begin{bmatrix} \mathbf{0} \\ \boldsymbol{\rho} p(t, \boldsymbol{\xi}) \end{bmatrix}. \tag{24}$$

The impulse response function $h_i(t)$ corresponding to the system in Eq. (23) is defined as:

$$h_i(t) = \sum_{r=1}^{2n_d} \frac{\boldsymbol{\beta}_i^T \boldsymbol{\Phi}_r \boldsymbol{\Upsilon}_{pr}^T \boldsymbol{\rho}}{(2\lambda_r T_r + S_r)} e^{\lambda_r t}, \tag{25}$$

where $i = 1, 2, \ldots, n_r$ denotes the number of responses, and $\boldsymbol{\beta}_i$ is a constant vector such that a response of interest η_i is generated as $\eta_i = \beta_i^T \boldsymbol{q}$. Variables T_r and S_r are the modal energies given by:

$$T_r = \boldsymbol{\Upsilon}_{pr}^T (\mathbf{M} + \mathbf{M}_e) \boldsymbol{\Phi}_{pr}, \quad S_r = \boldsymbol{\Upsilon}_{pr}^T (\mathbf{C} + \mathbf{C}_e) \boldsymbol{\Phi}_{pr}, \tag{26}$$

where $\boldsymbol{\Upsilon}_{pr}$ and $\boldsymbol{\Phi}_{pr}$ are, respectively, the position parts (i.e., the last n_d components) of the right and left eigenvectors, associated with the right and left eigenproblems of Eq. (23); λ_r contains the corresponding eigenvalues.

The dynamic responses $\boldsymbol{\eta}_i, i = 1, 2, \ldots, n_\eta$, that solve Eq. (1) are calculated by applying the convolution integral between the corresponding unit impulse response functions $h_i(t)$, $i = 1, 2, \ldots, n_\eta$, and the stochastic loading $p(t, \boldsymbol{\xi})$, i.e.:

$$\boldsymbol{\eta}_i(t, z) = \int_0^t h_i(t - \tau)\, p(t, \boldsymbol{\xi}) d\tau, \; i = 1, 2, \ldots, n_\eta. \tag{27}$$

In view of the excitation model introduced in Eq. (4), evaluating Eq. (27) at time t_k yields:

$$\boldsymbol{\eta}_i(t_k, \boldsymbol{\xi}) = \sum_{l_1=1}^{k} \Delta t \epsilon_{l_1} h_i(t_k - t_{l_1}) \left(\sum_{l_2=1}^{n_{KL}} \psi_{l_1, l_2} \sqrt{\lambda_{l_2}} \xi_{l_2} \right) = \boldsymbol{\gamma}_{i,k} \boldsymbol{\xi}, \tag{28}$$

for $i = 1, 2, \ldots, n_\eta$, $k = 1, 2, \ldots, n_T$, where ψ_{l_1, l_2} is the (l_1, l_2)-th element of matrix $\boldsymbol{\Psi}$; $\boldsymbol{\gamma}_{i,k}$ is a

n_{KL}-dimensional vector such that:

$$\boldsymbol{\gamma}_{i,k} = \left[\sum_{l_1=1}^{k} \Delta t \epsilon_{l_1} h_i(t_k - t_{l_1}) \psi_{l_1,1} \sqrt{\lambda_1} \quad \dots \quad \sum_{l_1=1}^{k} \Delta t \epsilon_{l_1} h_i(t_k - t_{l_1}) \psi_{l_1,n_{KL}} \sqrt{\lambda_{n_{KL}}} \right] \tag{29}$$

and ϵ_{l_1} is a coefficient depending on the numerical integration scheme used in the evaluation of the convolution integral. When the trapezoidal integration rule is chosen (Gautschi 2012), $\epsilon_{l_1} = 1/2$, if $l_1 = 1$ or $l_1 = k$; otherwise, $\epsilon_{l_1} = 1$. As such, $\boldsymbol{\eta}_i$ is calculated as a linear transformation that maps the standard normal random vector $\boldsymbol{\xi}$ to the responses $\boldsymbol{\eta}_i$ for each time instant:

$$\boldsymbol{\eta}_i(\boldsymbol{\xi}) = \boldsymbol{\Gamma}_i(\boldsymbol{\theta})\boldsymbol{\xi}, \tag{30}$$

where:

$$\boldsymbol{\Gamma}_i(\boldsymbol{\theta}) = \begin{bmatrix} \boldsymbol{\gamma}_{i,1}(\boldsymbol{\theta}) \\ \boldsymbol{\gamma}_{i,2}(\boldsymbol{\theta}) \\ \vdots \\ \boldsymbol{\gamma}_{i,n_T}(\boldsymbol{\theta}) \end{bmatrix} \tag{31}$$

is a $n_T \times n_{KL}$ matrix, which represents a linear map from the standard normal random vector $\boldsymbol{\xi}$ to the i-th response of interest. Note that $\boldsymbol{\Gamma}_i(\boldsymbol{\theta})$ depends directly on the epistemic uncertain parameters $\boldsymbol{\theta}$ through the eigenvalues and eigenvectors of the KL series expansion. Finally, it is highlighted that since the mean square linearization scheme is adopted (see Eq. (18)), an approximate solution is sought for the probability of failure, as computed by the linearized system shown in Eq. (30), rather than the exact solution. It is also highlighted that since the linearization is performed in a mean-squared error sense, it is known that the approximation of the true system is less accurate in the tails of the distribution. Hence, the accuracy of the method degenerates when considering smaller failure probabilities. However, as it is shown in the numerical examples section, the significant advantage of the herein proposed framework is that the probability of failure is computed in a less (computational) intensive manner. As such, the method allows the analyst to identify those areas in the hypercubic space $\boldsymbol{\theta}^I$ that yield an extremum in P_f, as well as get an initial estimate of the

effect of the epistemic uncertainty on the bounds of P_f.

Bounds on the first excursion probability

As explained in section "Linear problems", the operator norm theorem can be used to bound the probability of failure of linear models under epistemic uncertainty in the definition of the load. To extend the method towards treating nonlinear dynamical simulation models, a framework based on the combination of the operator norm-based treatment and the statistical linearization methodology is proposed (see also section "Linear problems"). Hereto, the linearized system of Eq. (30) is considered. Specifically, the epistemic uncertain parameters of the imprecisely defined stochastic load that bound P_f are defined as:

$$\boldsymbol{\theta}^U = \underset{\boldsymbol{\theta}\in\boldsymbol{\theta}^I}{\operatorname{argmax}} \max_{i=1,2,\ldots,n_\eta} \|\boldsymbol{\Gamma}_i(\boldsymbol{\theta})\|_{\infty,2} \tag{32}$$

and:

$$\boldsymbol{\theta}^L = \underset{\boldsymbol{\theta}\in\boldsymbol{\theta}^I}{\operatorname{argmin}} \max_{i=1,2,\ldots,n_\eta} \|\boldsymbol{\Gamma}_i(\boldsymbol{\theta})\|_{\infty,2}, \tag{33}$$

with $\boldsymbol{\Gamma}_i$ as defined in Eq. (31). These parameter realizations are used for finding the parameters that yield $\overline{P}_f$ and $\underline{P}_f$, respectively. Note that the explicit dependence of $\boldsymbol{\Gamma}_i$ is highlighted in these equations. The parameters $\boldsymbol{\theta}$ influence $\boldsymbol{\Gamma}_i$ through the eigenfunctions and corresponding eigenvalues of the KL expansion shown in Eq. (4) and the interaction with the structural nonlinearities. Based on the derivations in Tropp (2004), Eqs. (32) and (33) are recast into:

$$\boldsymbol{\theta}^U = \underset{\boldsymbol{\theta}\in\boldsymbol{\theta}^I,}{\operatorname{argmax}} \max_{i=1,2,\ldots,n_\eta} \max_{j=1,2,\ldots,n_T} \|\boldsymbol{\Gamma}_i^{j:}(\boldsymbol{\theta})\|_2 \tag{34}$$

and:

$$\boldsymbol{\theta}^L = \underset{\boldsymbol{\theta}\in\boldsymbol{\theta}^I}{\operatorname{argmin}} \max_{i=1,2,\ldots,n_\eta} \max_{j=1,2,\ldots,n_T} \|\boldsymbol{\Gamma}_i^{j:}(\boldsymbol{\theta})\|_2, \tag{35}$$

respectively, where the superscript '$j:$' denotes the j-th row of matrix $\boldsymbol{\Gamma}_i$ and $\|\cdot\|_2$ denotes the regular L_2 vector norm.

To summarize, the proposed procedure can be described as follows:

1. Represent the nonlinear model including the epistemic uncertainty by using Eq. (7).
2. Solve the optimization problems in Eqs. (34) and (35) to identify $\boldsymbol{\theta}^U$ and $\boldsymbol{\theta}^L$, by using any appropriate algorithm. Then, compute matrix $\boldsymbol{\Gamma}(\boldsymbol{\theta})$ for a given realization $\boldsymbol{\theta}$. This is done in two steps. First, applying the statistical linearization method, solve iteratively Eqs. (19)-(22). Secondly, taking into account Eqs. (24)-(31), perform modal analysis over the equivalent linear system to derive matrix $\boldsymbol{\Gamma}(\boldsymbol{\theta})$.
3. Once $\boldsymbol{\theta}^U$ and $\boldsymbol{\theta}^L$ are identified, perform reliability analysis using the full nonlinear model in order to determine the upper and lower bounds of the failure probability.

NUMERICAL EXAMPLES

Case study 1: two-degrees-of-freedom nonlinear system

In this case study, the two-degrees-of-freedom (DOF) system in Fig. 1 is considered. The system consists of masses m_1 and m_2, which are connected to each other by a linear damper of damping coefficient c_2 and a linear spring of stiffness coefficient k_2. Further, mass m_1 connects to the foundation by a linear damper of damping coefficient c_1 and a nonlinear spring of stiffness coefficient k_1.

Next, considering the coordinates vector $\mathbf{q}^{\mathrm{T}} = \begin{bmatrix} q_1 & q_2 \end{bmatrix}$ and following the standard Newtonian approach to derive the system governing equations of motion (Roberts and Spanos 2003), Eq. (1) is formulated. The system parameter matrices are given by:

$$\mathbf{M} = \begin{bmatrix} m_1 & 0 \\ 0 & m_2 \end{bmatrix}, \ \mathbf{C} = \begin{bmatrix} c_1 + c_2 & -c_2 \\ -c_2 & c_2 \end{bmatrix}, \ \mathbf{K} = \begin{bmatrix} k_1 + k_2 & -k_2 \\ -k_2 & k_2 \end{bmatrix}, \tag{36}$$

whereas:

$$\boldsymbol{\rho} p(t, \boldsymbol{\xi}) = \begin{bmatrix} 1 \\ 0 \end{bmatrix} p_1(t, \boldsymbol{\xi}) \tag{37}$$

denotes the stochastic excitation. Further, the nonlinear restoring force of the system is given by:

$$\mathbf{\Phi}(\ddot{\mathbf{q}}, \dot{\mathbf{q}}, \mathbf{q}) = \begin{bmatrix} k_1 \nu q_1^3 \\ 0 \end{bmatrix}, \tag{38}$$

where ν corresponds to the intensity of the nonlinearity. Finally, the load $p(t, \boldsymbol{\xi})$ acting on the system is modeled as a zero-mean Gaussian stochastic process, described by the Clough-Penzien spectrum (Li and Chen 2009):

$$S_{PP}(\omega) = \frac{\omega^4 \left(\omega_g^4 + (2\zeta_g \omega_g \omega)^2\right) S_0}{\left((\omega_g^2 - \omega^2)^2 + (2\zeta_g \omega_g \omega)^2\right)\left((\omega_f^2 - \omega^2)^2 + (2\zeta_f \omega_f \omega)^2\right)}. \tag{39}$$

The following parameter values are considered for the system in Fig. 1, $m_1 = m_2 = 1$ [kg], $c_1 = c_2 = 0.2$ [N· s/m], $k_1 = k_2 = 1$ [N/m], whereas the intensity of the nonlinearity is $\nu = 1$ and the nominal parameters of the excitation spectrum are $[\omega_g, \omega_f, \zeta_g, \zeta_f, S_0] = [4\pi, 0.4\pi, 0.7, 0.7, 3 \times 10^{-4}]$. Failure of the system is considered as the first passage of any of the displacements of the masses over a threshold value of $b = 0.040$ [m]. In this regard, the nonlinear system is solved by employing an iterative Newmark solver for obtaining the response displacement $\mathbf{q}$ for every realization of the stochastic load process. Given the difficulty in determining the failure domain for this particular nonlinear system, Eq. (5) is approximated using plain Monte Carlo sampling with a sample size of 5000 samples. ~~This is warranted since the probability of failure of the system with the considered threshold b has an order of magnitude of 10^{-1}.~~ Further, it is considered that the analyst is unsure about the exact values of the stochastic load acting on the system. Specifically, the definition of the parameters of the Clough-Penzien spectrum is subject to epistemic uncertainty. The intervals that are applied for bounding this epistemic uncertainty are shown in Table 1.

Next, the herein proposed operator norm theory-based statistical linearization framework is employed for computing the bounds on the probability of failure. In this regard, first, the governing equation of motion with parameter matrices and nonlinear vector given by Eqs. (36) and Eq. (38), respectively, is replaced by an equivalent linear system of the form of Eq. (17). Then, considering

the error function in Eq. (18) and adopting a mean square minimization of the error, Eq. (19) leads to the equivalent parameter matrices:

$$\mathbf{M}_e = \begin{bmatrix} 0 & 0 \\ 0 & 0 \end{bmatrix}, \quad \mathbf{C}_e = \begin{bmatrix} 0 & 0 \\ 0 & 0 \end{bmatrix}, \quad \mathbf{K}_e = \begin{bmatrix} 3k_1\nu\sigma_{q_1}^2 & 0 \\ 0 & 0 \end{bmatrix}. \tag{40}$$

Regarding the numerical implementation, considering as stopping criterion $\left|\frac{\mathbf{K}_e^{i+1}-\mathbf{K}_e^i}{\mathbf{K}_e^i}\right| < 10^{-5}$, where the index '$i$' denotes the i-th iteration and the initial value $\mathbf{K}_e^0$ is set equal to zero, the iterative scheme described in the section "Statistical linearization methodology" converges after three iterations. Thus, the nonlinear system shown in Fig. 1 is approximated by the equivalent linear system whose governing equations of motion are given by Eq. (17).

Next, the augmented state-space system in Eq. (23) is formulated and taking into account Eqs. (25)-(30), the linear map $\mathbf{\Gamma}_i(\boldsymbol{\theta})$ is calculated. Then, following the presentation in the section "Bounds on the first excursion probability", and considering the derived equivalent linear matrices, the operator norm that corresponds to a certain realization of the epistemically uncertain Gaussian process load is computed. In addition, the optimization over the operator norm is performed using the Matlab built-in patternsearch optimization tool. Finally, two optimization problems have to be solved; the first one for determining $\boldsymbol{\theta}^U$ (see Eq. (34)) and the second one for determining $\boldsymbol{\theta}^L$ (see Eq. (35)), which require approximately 100 iterations to converge.

So far, the operator norm-based statistical linearization framework is used for determining the bounds on P_f. Next, the validity of the obtained results is verified by using a brute-force implementation of the double-loop problem. Hereto, the Newmark solver is considered in conjunction with Monte Carlo simulation (MCS) as the 'inner loop' in Eqs. (8) and (9) for computing P_f for each realization of the epistemic uncertainty. A patternsearch optimization algorithm (Kolda et al. 2003) is used to solve the optimization problem in the 'outer loop'. This result serves as the benchmark for the bounds on P_f against which the result of the proposed operator norm-based statistical linearization framework is compared.

Results and discussion

The functional relationship between the operator norm $\|\mathbf{\Gamma}\|_{2,\infty}$, as computed over the linearized system, and P_f, as computed using MCS combined with the Newmark solver, is shown in Fig. 2. The blue dots in this figure are obtained by drawing 640 uniformly distributed samples in between the bounds of $\boldsymbol{\theta}^I$. First, it is noted that the relation between the operator norm $\|\mathbf{\Gamma}_i(\boldsymbol{\theta})\|_{\infty,2}$ and P_f is not bijective. This is explained by the fact that the operator norm combines failure phenomena of several responses at the same time, and consists of a potentially complicated interaction between the natural frequencies of the structure under consideration and the dominant frequencies of the load that acts on the system (Faes et al. 2021b). Furthermore, it is readily seen that the extreme values in P_f and $\|\mathbf{\Gamma}\|_{2,\infty}$ are in good agreement, as also suggested in Table 2. In addition, there is a clear trend between these two quantities, where higher operator norm values correspond to higher probability of failure values and vice-versa. Note that Table 2 also reports on the combinations of crisp values associated with the epistemic uncertainty of the external loading that yield extreme values for the failure probability. It is important to stress that to obtain a value for the operator norm, only the linear map $\mathbf{\Gamma}$ (see Eq. (30)) needs to be assembled and the corresponding operator norm needs to be calculated. On the other hand, the calculation of one value of P_f requires the full solution of Eq. (5). ~~As such, the computational gain is even larger than suggested in Table 2, since the 520 evaluations of the operator norm during the minimizing did not require the system matrices to be re-evaluated.~~

Case study 2: six degrees-of-freedom structure

In this example, a 6-DOF system of rigid masses m_i $(i = 1, 2, \cdots, 6)$ connected to each other by nonlinear dampers as shown in Fig. 3 is considered. In this regard, considering the coordinates vector $\mathbf{q}^{\mathrm{T}} = \begin{bmatrix} q_1 & q_2 & q_3 & q_4 & q_5 & q_6 \end{bmatrix}$, the matrix form of the system governing equations of

motion is formulated (see Eq. (1)), whose parameter matrices are given by:

$$\mathbf{M} = \begin{bmatrix} m_1 & 0 & 0 & 0 & 0 & 0 \\ m_2 & m_2 & 0 & 0 & 0 & 0 \\ m_3 & m_3 & m_3 & 0 & 0 & 0 \\ m_4 & m_4 & m_4 & m_4 & 0 & 0 \\ m_5 & m_5 & m_5 & m_5 & m_5 & 0 \\ m_6 & m_6 & m_6 & m_6 & m_6 & m_6 \end{bmatrix}, \mathbf{C} = \begin{bmatrix} c_1 & -c_2 & 0 & 0 & 0 & 0 \\ 0 & c_2 & -c_3 & 0 & 0 & 0 \\ 0 & 0 & c_3 & -c_4 & 0 & 0 \\ 0 & 0 & 0 & c_4 & -c_5 & 0 \\ 0 & 0 & 0 & 0 & c_5 & -c_6 \\ 0 & 0 & 0 & 0 & 0 & c_6 \end{bmatrix} \tag{41}$$

and:

$$\mathbf{K} = \begin{bmatrix} k_1 & -k_2 & 0 & 0 & 0 & 0 \\ 0 & k_2 & -k_3 & 0 & 0 & 0 \\ 0 & 0 & k_3 & -k_4 & 0 & 0 \\ 0 & 0 & 0 & k_4 & -k_5 & 0 \\ 0 & 0 & 0 & 0 & k_5 & -k_6 \\ 0 & 0 & 0 & 0 & 0 & k_6 \end{bmatrix}. \tag{42}$$

Further, it is assumed that the system is subjected to ground acceleration, which is modeled as a stochastic process applied to masses m_1 to m_6. The corresponding power spectrum is given by:

$$\mathbf{S}(\omega) = \begin{bmatrix} S_1(\omega) & 0 & 0 & 0 & 0 & 0 \\ 0 & S_2(\omega) & 0 & 0 & 0 & 0 \\ 0 & 0 & S_3(\omega) & 0 & 0 & 0 \\ 0 & 0 & 0 & S_4(\omega) & 0 & 0 \\ 0 & 0 & 0 & 0 & S_5(\omega) & 0 \\ 0 & 0 & 0 & 0 & 0 & S_6(\omega) \end{bmatrix}, \tag{43}$$

where $S_i(\omega)$, $i = 1, 2, \ldots, 6$, is modeled as a Clough-Penzien spectrum (see Eq. (39)) with the epistemic uncertainty on the parameters ω_g, ω_f, ζ_g and ζ_f characterized by the intervals given in Table 1, whereas the parameter S_0 is characterized by the interval $[0.8, 1.2] \times 0.05$. In addition,

the nonlinear function $\mathbf{\Phi}(\ddot{\mathbf{q}}, \dot{\mathbf{q}}, \mathbf{q})$ takes the form:

$$\mathbf{\Phi}^{\mathrm{T}}(\ddot{\mathbf{q}}, \dot{\mathbf{q}}, \mathbf{q}) = \left[c_1 \nu \dot{q}_1^3 - c_2 \nu \dot{q}_2^3 \quad c_2 \nu \dot{q}_2^3 - c_3 \nu \dot{q}_3^3 \quad c_3 \nu \dot{q}_3^3 - c_4 \nu \dot{q}_4^3 \quad c_4 \nu \dot{q}_4^3 - c_5 \nu \dot{q}_5^3 \quad c_5 \nu \dot{q}_5^3 - c_6 \nu \dot{q}_6^3 \quad c_6 \nu \dot{q}_6^3\right], \tag{44}$$

with ν describing the intensity of the nonlinearity in Eq. (44). The system parameter values are $m_1 = m_2 \cdots = m_6 = 1$, $c_1 = c_2 \cdots = c_6 = 0.2$, $k_1 = k_2 \cdots = k_6 = 1$ and $\nu = 3$. Finally, failure is defined in this case when any inter-story drift exceeds the maximum allowable threshold $b = 0.6$ m during the entire analysis period.

Then, the herein proposed operator norm theory-based statistical linearization framework is applied. In this regard, the equivalent linear mass and stiffness 6×6 matrices take the form:

$$\mathbf{M_e} = \mathbf{K_e} = \mathbf{0}, \tag{45}$$

whereas the equivalent linear damping 6×6 matrix becomes:

$$\mathbf{C_e} = \begin{bmatrix} 3c_1\nu\sigma_{\dot{q}_1}^2 & -3c_2\nu\sigma_{\dot{q}_2}^2 & 0 & 0 & 0 & 0 \\ 0 & 3c_2\nu\sigma_{\dot{q}_2}^2 & -3c_3\nu\sigma_{\dot{q}_3}^2 & 0 & 0 & 0 \\ 0 & 0 & 3c_3\nu\sigma_{\dot{q}_3}^2 & -3c_4\nu\sigma_{\dot{q}_4}^2 & 0 & 0 \\ 0 & 0 & 0 & 3c_4\nu\sigma_{\dot{q}_4}^2 & -3c_5\nu\sigma_{\dot{q}_5}^2 & 0 \\ 0 & 0 & 0 & 0 & 3c_5\nu\sigma_{\dot{q}_5}^2 & -3c_6\nu\sigma_{\dot{q}_6}^2 \\ 0 & 0 & 0 & 0 & 0 & 3c_6\nu\sigma_{\dot{q}_6}^2 \end{bmatrix}. \tag{46}$$

The elements of the equivalent matrix in Eq. (46) are determined by utilizing the iterative scheme described in the section "Statistical linearization methodology". Specifically, using $\left|\frac{\mathbf{C}_e^{i+1} - \mathbf{C}_e^i}{\mathbf{C}_e^i}\right| < 10^{-5}$ as stopping criterion, where 'i' denotes the i-th iteration of the scheme, and also considering the initial value $\mathbf{C}_e^0 = \mathbf{0}$, the scheme converges after five iterations. Thus, the nonlinear system shown

in Fig. 3 is approximated by the equivalent linear system whose governing equations of motion are given by Eq. (17).

Next, the augmented state-space system in Eq. (23) is formulated and taking into account Eqs. (25)-(30), the linear map $\mathbf{\Gamma}_i(\boldsymbol{\theta})$ is calculated. Subsequently, following the presentation in the section "Bounds on the first excursion probability", and considering the derived equivalent linear matrices, the operator norm that corresponds to a certain realization of the epistemically uncertain Gaussian process load is computed. In addition, the optimization over the operator norm is performed using the Matlab built-in patternsearch optimization tool. Finally, two optimization problems have to be solved; the first one for determining $\boldsymbol{\theta}^U$ (see Eq. (34)) and the second one for determining $\boldsymbol{\theta}^L$ (see Eq. (35)), which require approximately 200 iterations to converge.

Results and discussion

The results of the herein proposed norm operator-based statistical linearization framework are shown in Table 3. Clearly, the proposed method is capable of adequately approximating the true bounds on P_f. The results are compared to a brute-force double loop implementation using Newmark method to solve the nonlinear ODE, MCS to calculate P_f, and patternsearch in Matlab to optimize over the epistemic parameter space. It is highlighted that the results obtained by following the proposed approach are in reasonable agreement with the corresponding results obtained by following a classic double loop approach. The small discrepancy between the results is expected and is due to adopting an approximate linearization scheme to enable the application of the operator norm framework. Yet, given the large gain in computational efficiency, the small loss in accuracy is warranted. Nonetheless, it can be argued that these bounds are highly reasonable given the immense reduction in computational cost that is required to calculate them. For instance, considering the upper bound on P_f, the required number of deterministic model solutions can be reduced from 292.000 to just 626, with an additional 1000 samples for computing the associated failure probability.

CONCLUSIONS

In this paper, a novel technique has been developed for bounding the responses and probability

of failure of nonlinear models subjected to imprecisely defined stochastic loads. The proposed technique can be construed as a generalization of a recently developed operator norm-based method to account for nonlinear dynamical systems. This is attained by resorting to the statistical linearization approximate methodology for defining a linear system equivalent to the nonlinear system under consideration. In this regard, the double loop that is typically associated with estimating the bounds on the probability of failure of nonlinear dynamical systems is effectively decoupled and the associated computational cost is reduced by several orders of magnitude. Thus, it can be argued that integrating statistical linearization into the operator norm framework allows for bounding the probability of failure of nonlinear systems with acceptable accuracy and at greatly reduced cost. It is noted, however, that since the linearization scheme has been performed in a mean-square error minimization sense, the representation of the nonlinear system is less accurate in the tails of the distribution. This aspect renders the proposed approach mostly suitable for estimating the bounds of moderate to large failure probabilities. Nevertheless, future work is directed towards developing an enhanced operator norm-based linearization scheme capable of estimating bounds on smaller failure probabilities, as well as towards integrating the proposed framework with more advanced simulation methods, such as importance sampling or subset simulation. The validity and numerical efficiency of the proposed technique has been demonstrated by considering two nonlinear structural systems.

DATA AVAILABILITY STATEMENT

Some or all data, models, or code that support the findings of this study are available from the corresponding author upon reasonable request.

ACKNOWLEDGMENTS

The authors gratefully acknowledge the support and funding from the German Research Foundation under Grant No. BE 2570/7-1 & MI 2459/1-1; from ANID (National Agency for Research and Development, Chile) and DAAD (German Academic Exchange Service) under CONICYT-PFCHA/Doctorado Acuerdo Bilateral DAAD Becas Chile/2018-6218007. Matthias Faes further

529 acknowledges the financial support of the Research Foundation Flanders (FWO) under post-doc
530 grant 12P3519N, as well as the Alexander von Humboldt foundation. Marcos Valdebenito ac-
531 knowledges the support by ANID (National Agency for Research and Development, Chile) under
532 its program FONDECYT, grant number 1180271.

533 **REFERENCES**

534 Au, S. (2009). "Stochastic control approach to reliability of elasto-plastic structures." Journal Of
535 Structural Engineering and Mechanics, 32(1), 21–36.

536 Beer, M. (2004). "Uncertain structural design based on nonlinear fuzzy analysis." Journal of
537 Applied Mathematics and Mechanics (ZAMM), 84(10-11), 740–753.

538 Beer, M., Ferson, S., and Kreinovich, V. (2013). "Imprecise probabilities in engineering analyses."
539 Mechanical Systems and Signal Processing, 37(1-2), 4–29.

540 Betz, W., Papaioannou, I., and Straub, D. (2014). "Numerical methods for the discretization of
541 random fields by means of the Karhunen-Loève expansion." Computer Methods in Applied
542 Mechanics and Engineering, 271, 109–129.

543 Chen, J. and Li, J. (2013). "Optimal determination of frequencies in the spectral representation of
544 stochastic processes." Computational Mechanics, 51(5), 791–806.

545 Chopra, A. (1995). Dynamics of structures: theory and applications to earthquake engineering.
546 Prentice Hall.

547 de Angelis, M., Patelli, E., and Beer, M. (2015). "Advanced line sampling for efficient robust
548 reliability analysis." Structural Safety, 52, Part B, 170–182.

549 Elishakoff, I. and Andriamasy, L. (2012). "The tale of stochastic linearization technique: Over half
550 a century of progress." Nondeterministic mechanics, 115–189.

551 Faes, M. and Moens, D. (2019a). "Imprecise random field analysis with parametrized kernel
552 functions." Mechanical Systems and Signal Processing, 134, 106334.

553 Faes, M. and Moens, D. (2019b). "Recent Trends in the Modeling and Quantification of Non-
554 probabilistic Uncertainty." Archives of Computational Methods in Engineering.

555 Faes, M., Sadeghi, J., Broggi, M., de Angelis, M., Patelli, E., Beer, M., and Moens, D. (2019). "On
556 the Robust Estimation of Small Failure Probabilities for Strong Nonlinear Models." ASCE-ASME
557 J Risk and Uncert in Engrg Sys Part B Mech Engrg, 5(4).

558 Faes, M. and Valdebenito, M. (2021). "Fully decoupled reliability-based optimization of lin-
559 ear structures subject to gaussian dynamic loading considering discrete design variables."
560 Mechanical Systems and Signal Processing, 156, 107616.

561 Faes, M. G. and Valdebenito, M. A. (2020). "Fully decoupled reliability-based design optimization
562 of structural systems subject to uncertain loads." Computer Methods in Applied Mechanics and
563 Engineering, 371, 113313.

564 Faes, M. G., Valdebenito, M. A., Moens, D., and Beer, M. (2020). "Bounding the first excur-
565 sion probability of linear structures subjected to imprecise stochastic loading." Computers &
566 Structures, 239, 106320.

567 Faes, M. G. R., Daub, M., Marelli, S., Patelli, E., and Beer, M. (2021a). "Engineering analysis with
568 probability boxes : a review on computational methods." Structural Safety.

569 Faes, M. G. R., Valdebenito, M. A., Moens, D., and Beer, M. (2021b). "Operator norm theory as an
570 efficient tool to propagate hybrid uncertainties and calculate imprecise probabilities." Mechanical
571 Systems and Signal Processing.

572 Fragkoulis, V. C., Kougioumtzoglou, I. A., and Pantelous, A. A. (2016). "Statistical linearization of
573 nonlinear structural systems with singular matrices." Journal of Engineering Mechanics, 142(9),
574 04016063.

575 Fragkoulis, V. C., Kougioumtzoglou, I. A., Pantelous, A. A., and Beer, M. (2019). "Non-stationary

response statistics of nonlinear oscillators with fractional derivative elements under evolutionary stochastic excitation." Nonlinear Dynamics, 97(4), 2291–2303.

Gautschi, W. (2012). Numerical Analysis. Birkhäuser Boston, 2nd edition.

Imholz, M., Faes, M., Vandepitte, D., and Moens, D. (2020). "Robust uncertainty quantification in structural dynamics under scarse experimental modal data: A bayesian-interval approach." Journal of Sound and Vibration, 467, 114983.

Jensen, H. and Valdebenito, M. (2007). "Reliability analysis of linear dynamical systems using approximate representations of performance functions." Structural Safety, 29(3), 222–237.

Kolda, T., Lewis, R., and torczon, V. (2003). "Optimization by direct search: New perspectives on some classical and modern methods." SIAM Review, 45(3), 385–482.

Kougioumtzoglou, I., Fragkoulis, V., Pantelous, A., and Pirrotta, A. (2017). "Random vibration of linear and nonlinear structural systems with singular matrices: A frequency domain approach." Journal of Sound and Vibration, 404, 84–101.

Lee, J. and Verleysen, M. (2007). Nonlinear Dimensionality Reduction. Springer.

Li, J. and Chen, J. (2009). Stochastic dynamics of structures. John Wiley & Sons.

Moens, D. and Vandepitte, D. (2004). "An interval finite element approach for the calculation of envelope frequency response functions." International Journal for Numerical Methods in Engineering, 61(14), 2480–2507.

Ni, P., Fragkoulis, V. C., Kong, F., Mitseas, I. P., and Beer, M. (2021). "Response determination of nonlinear systems with singular matrices subject to combined stochastic and deterministic excitations." ASCE-ASME Journal of Risk and Uncertainty in Engineering Systems, Part A: Civil Engineering, 7(4), 04021049.

Pasparakis, G., Fragkoulis, V., and Beer, M. (2021). "Harmonic wavelets based response evolutionary power spectrum determination of linear and nonlinear structural systems with singular matrices." Mechanical Systems and Signal Processing, 149, 107203.

Pradlwarter, H., Schuëller, G., Koutsourelakis, P., and Charmpis, D. (2007). "Application of line sampling simulation method to reliability benchmark problems." Structural Safety, 29(3), 208–221.

Roberts, J. B. and Spanos, P. D. (2003). Random vibration and statistical linearization. Courier Corporation.

Schenk, C. and Schuëller, G. (2005). Uncertainty Assessment of Large Finite Element Systems. Springer-Verlag, Berlin/Heidelberg/New York.

Schöbi, R. and Sudret, B. (2017). "Structural reliability analysis for p-boxes using multi-level meta-models." Probabilistic Engineering Mechanics, 48, 27–38.

Schuëller, G. and Pradlwarter, H. (2007). "Benchmark study on reliability estimation in higher dimensions of structural systems – An overview." Structural Safety, 29, 167–182.

Shinozuka, M. and Sato, Y. (1967). "Simulation of nonstationary random process." Journal of the Engineering Mechanics Division, 93(1), 11–40.

Socha, L. (2007). Linearization methods for stochastic dynamic systems, Vol. 730. Springer Science & Business Media.

Spanos, P. D., Di Matteo, A., Cheng, Y., Pirrotta, A., and Li, J. (2016). "Galerkin scheme-based determination of survival probability of oscillators with fractional derivative elements." Journal of Applied Mechanics, 83(12).

Spanos, P. D. and Kougioumtzoglou, I. A. (2014). "Survival probability determination of nonlinear oscillators subject to evolutionary stochastic excitation." Journal of Applied Mechanics, 81(5).

Spanos, P. D. and Malara, G. (2020). "Nonlinear vibrations of beams and plates with fractional derivative elements subject to combined harmonic and random excitations." Probabilistic Engineering Mechanics, 59, 103043.

Stefanou, G. (2009). "The stochastic finite element method: Past, present and future." Computer Methods in Applied Mechanics and Engineering, 198(9-12), 1031–1051.

Tropp, J. A. (2004). "Topics in Sparse Approximation." Ph.D. thesis, The University of Texas at Austin, , <http://www.lib.utexas.edu/etd/d/2004/troppd73287/troppd73287.pdf>.

Vanmarcke, E. and Grigoriu, M. (1983). "Stochastic finite element analysis of simple beams." Journal of Engineering Mechanics, 109(5).

Wei, P., Liu, F., Valdebenito, M., and Beer, M. (2021). "Bayesian probabilistic propagation of imprecise probabilities with large epistemic uncertainty." Mechanical Systems and Signal Processing, 149, 107219.

Wei, P., Song, J., Bi, S., Broggi, M., Beer, M., Lu, Z., and Yue, Z. (2019). "Non-intrusive stochastic analysis with parameterized imprecise probability models: I. performance estimation." Mechanical Systems and Signal Processing, 124, 349 – 368.

List of Tables

TABLE 1. Tested values for $\boldsymbol{\theta}^I$.

ω_g^I	ω_f^I	ζ_g^I	ζ_f^I	S_0^I
$[0.8, 1.2] \times 4\pi$	$[0.8, 1.2] \times 0.4\pi$	$[0.8, 1.2] \times 0.7$	$[0.8, 1.2] \times 0.7$	$[0.8, 1.2] \times 3 \times 10^{-4}$

TABLE 2. Results of the optimization problems. Case study 1.

parameter	$\underline{P_f}$ (DL)	$\underline{P_f}$ (ON)	$\overline{P}_f$ (DL)	$\overline{P}_f$ (ON)
S_0^*	$2.409 \cdot 10^{-04}$	$2.409 \cdot 10^{-04}$	$3.591 \cdot 10^{-04}$	$3.591 \cdot 10^{-04}$
ω_g^*	10.316	15.080	13.969	10.056
ω_f^*	1.507	1.508	1.007	1.005
ζ_g^*	0.700	0.840	0.825	0.840
ζ_f^*	0.825	0.840	0.576	0.560
P_f	0.090	0.083	0.969	0.969
ON	0.0072	0.0069	0.0360	0.0375
n^0	2010000	520 + 5000	225500	595 + 5000

TABLE 3. Results of the optimization problems. Case study 2.

parameter	$\underline{P_f}$ (DL)	$\underline{P_f}$ (ON)	$\overline{P}_f$ (DL)	$\overline{P}_f$ (ON)
S_0^*	0.040	0.040	0.060	0.060
ω_g^*	12.557	12.684	14.570	10.053
ω_f^*	1.507	1.508	1.007	1.005
ζ_g^*	0.809	0.840	0.700	0.560
ζ_f^*	0.827	0.840	0.567	0.560
P_f	0.097	0.123	0.859	0.855
ON	0.081	0.079	0.307	0.319
n^0	281000	1804 + 1000	292000	626 + 1000

List of Figures

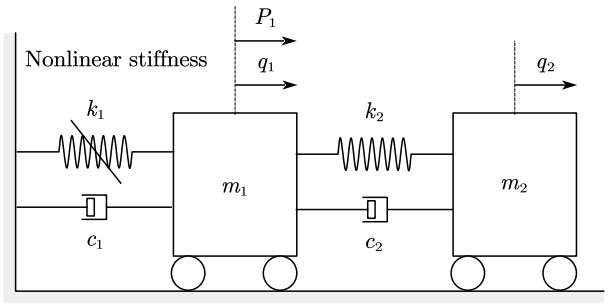

Fig. 1. A two-degrees-of-freedom nonlinear system under stochastic excitation.

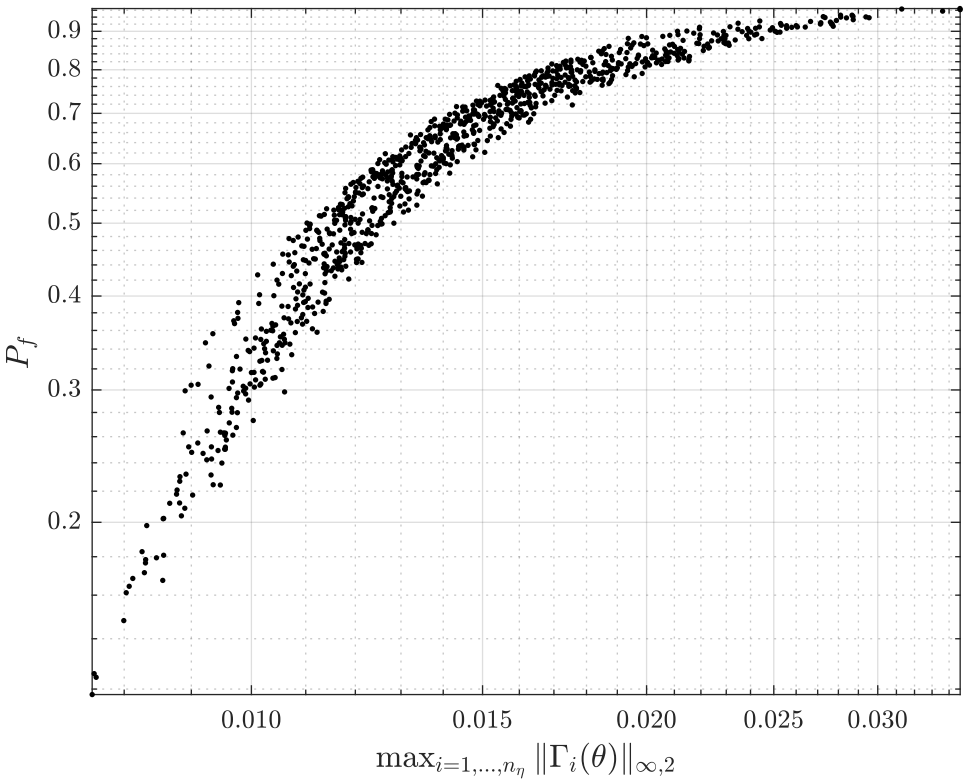

Fig. 2. Comparison of the operator norm, computed on the linearized system with the probability of failure as computed by Monte Carlo simulation in combination with Newmark method.

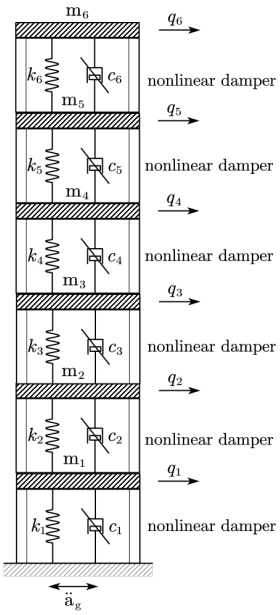

Fig. 3. A six-degrees-of-freedom nonlinear system under stochastic excitation.